2015

TAT-HSP70 ATTENUATES EXPERIMENTAL LUNG INJURY

M. M. Lyons

N. N. Raj

J. L. Chittams

L. Kilpatrick

C. S. Deutschman
Zucker School of Medicine at Hofstra/Northwell

Recommended Citation

TAT-HSP70 Attenuates Experimental Lung Injury

M. Melanie Lyons, BSN, MSN, PhD[1,2], **Nichelle N. Raj, BS**[1], **Jesse L. Chittams, MS**[2,5], **Laurie Kilpatrick, PhD**[3,4], and **Clifford S. Deutschman, MS, MD, FCCM**[1,2]

[1]Department of Anesthesiology and Critical Care, University of Pennsylvania Perelman School of Medicine, Philadelphia, Pennsylvania, USA

[2]University of Pennsylvania School of Nursing, Philadelphia, Pennsylvania, USA

[5]Biostatistics Consulting Unit, Office of Nursing Research, University of Pennsylvania, Philadelphia, Pennsylvania, USA

[3]Center for Inflammation, Translational and Clinical Lung Research, Temple University School of Medicine, Philadelphia, Pennsylvania, USA

[4]Department of Physiology, Temple University School of Medicine, Philadelphia, Pennsylvania, USA

Abstract

Sepsis, a poorly understood syndrome of disordered inflammation, is the leading cause of death in critically ill patients. Lung injury, in the form of the Acute Respiratory Distress Syndrome (ARDS), is the most common form of organ injury in sepsis. The Heat Shock Response, during which Heat Shock Proteins (HSPs) are expressed, is an endogenous mechanism to protect cells from injury. We have found that the abundance of pulmonary Heat Shock Protein 70 (HSP70) is not increased following cecal ligation and double puncture (CLP), a rat model of sepsis-induced ARDS. Using the HIV-1 Trans-Activator of Transcription (TAT) cell penetrating protein, we enhanced HSP70 protein abundance in the lung. We found that intra-tracheal (IT) administration of HSP70 using the TAT methodology, just after CLP (CLP-TAT-HSP70), when compared to treatment with phosphate buffered saline (PBS) (CLP-PBS), significantly increased HSP70 abundance in the lung 24 and 48 h post surgery. Treatment of septic rats with TAT-HSP70 increased HSP70 abundance in histologically normal and abnormal lung regions. In addition, TAT-HSP70 treatment significantly decreased the levels of Macrophage Inflammatory Protein (MIP) -2 and Cytokine Induced Neutrophil Chemoattractant (CINC) -1 24 h after CLP. TATHSP70 treatment reduced Myeloperoxidase abundance 48 h post-CLP and attenuated histological evidence of inflammation at both 24 and 48 h. Administration of TAT-HSP70 also improved 48 h survival in this rat model of sepsis. Thus, IT administration of TAT-HSP70 increased HSP70 abundance in the lung and attenuated the lung injury. Enhancing pulmonary HSP70 using TAT is a novel potential therapeutic strategy for the treatment of ARDS that will be explored further.

Author Manuscript

Keywords

Introduction

Sepsis, an often fatal syndrome of disordered inflammation, is the leading cause of death in the critically ill (1-3). Recent data indicate in excess of 1,000,000 new cases/year in the United States (1, 4). Mortality from sepsis-related syndromes is high, and survivors often have cognitive and musculoskeletal dysfunction and poor quality of life (4-7). Sepsis is especially prevalent among vulnerable populations such as the elderly (8). Treatment of this complex disorder is also expensive - sepsis care now costs the United States healthcare system in excess of $24 billion/year (9-12). Clearly, sepsis is a public health problem of enormous importance.

The lung is the organ most often affected by sepsis. Pulmonary dysfunction in sepsis, termed the Acute Respiratory Distress Syndrome (ARDS), may progress rapidly from mild to moderate to severe injury (13). While ARDS is most often initiated by pathology within the lung itself, it can also arise as a result of remote injury or infection, including intra-abdominal infection (14). ARDS is characterized pathologically by alveolar damage, interstitial and alveolar edema, altered blood flow and capillary disruption, and damage to Type I and II alveolar epithelial cells that in part reflect dysregulated inflammation with aberrant activation of neutrophils and macrophages (15-19). While early identification and protective ventilation strategies have reduced ARDS-associated mortality, the combination of significant mortality, life-altering disability in survivors and substantial financial implications mandate novel approaches to treatment (20, 21).

The Heat Shock Response (HSR) is a highly conserved endogenous mechanism that protects cells from injury. In the HSR, cells respond to a number of noxious stimuli by expressing Heat Shock Proteins (HSPs), polypeptides that regulate protein folding/unfolding, intracellular transport, denaturation/aggregation, and degradation (22). In previous work we have shown that expression of a family of HSPs with molecular weights around 70kDa (collectively are called HSP70) is diminished in the lungs of rats with sepsis-induced ARDS (23). Increasing HSP70 abundance using an adenoviral vector delivery system (AdHSP) significantly decreased lung injury in rats subjected to cecal ligation and double puncture (CLP) (24, 25). AdHSP also limited CLP-mediated activation of the transcription factor NF-κB, blocked caspase-induced death of Type I pulmonary epithelial cells and attenuated excessive cell division and proliferation of Type II pulmonary cells (26-28). However, use of adenoviral vectors has been associated with excessive inflammation in transduced cells, dysregulated triggering of inflammatory pathways, the development of excessive cytolytic responses and death (29). Thus, development of alternative delivery strategies to enhance HSP70 abundance in the lungs might be of immense value.

The Trans- Activator of Transcription (TAT), a non-toxic, non-infectious cell penetrating protein derived from the Type 1 HIV virus, is a potential protein delivery system (30, 31).

TAT has been used to introduce more than 50 proteins into cells, both *in vivo* and *in vitro* (32-34). We have previously attenuated CLP-induced lung injury in rats using the TAT protein to deliver an inhibitor of one isoform of protein kinase C (δPKC) into the lungs (35, 36). In this study, we hypothesize using the TAT delivery system to enhance intracellular HSP70 abundance in pulmonary cells of rats with lung injury secondary to CLP will have a similar effect to AdHSP.

Materials and Methods

Production of TAT-HSP70

The recombinant TAT-HSP70 fusion protein (gift of H. Wong MD, Cincinnati Children's Hospital) was introduced into a replication vector (Impact Pharmaceuticals, Swarthmore, PA) and was expressed in *Escherichia Coli* as previously described (37). The purity of the resulting protein was ~90%.

Animal Protocol and Induction of Sepsis

All animal experiments were approved by the University of Pennsylvania Institutional Animal Care and Use Committee and were conducted in an approved facility overseen by the University Laboratory Animal Resources Center. Studies were performed on male 8-12 week old Sprague-Dawley (SD) rats weighing 250 - 300 grams, (Charles River, Boston, Massachusetts, USA). Rats were housed in a climate controlled, 12 h light/12 h dark cycle facility and allowed free access to food and water. Previous studies have demonstrated that these animals reliably develop ARDS after CLP (23, 35, 36).

CLP was performed under 2% Isoflurane anesthesia as previously described (23). After ligation the cecum was punctured twice with an 18-gauge needle. In Sham Operated (SO) controls the cecum was manipulated but not ligated or punctured. Intra-tracheal (IT) instillation of TAT-HSP70 or phosphate buffered saline (PBS) (vehicle) was conducted via tracheotomy as previously described (24). In treated animals, 200μl of PBS containing 100 μg of TAT-HSP70 (CLP-TAT-HSP70) were injected into a tracheal cannula inserted through a small incision. A like volume of PBS alone was administered IT to control (CLP-PBS) animals. Injection was followed by 2 ml of air to assure equal distribution of agent into lungs (24). Immediately following surgery and every 24 h thereafter, both SO and CLP animals were fluid resuscitated with 50 ml/kg of 0.9% saline subcutaneously. Prior to intervention, specific rats in each of four interventional groups were designated for sacrifice at 24 or 48 h. At the appropriate time point, rats received an intra-peritoneal injection of pentobarbital (200mg/kg). The laparotomy incision was re-opened and the animals were exsanguinated via the abdominal inferior vena cava.

Previous studies have indicated that at least three surviving animals are required to provide sufficient data to determine significance (23). To assure sufficient numbers a total of 73 animals were studied (Table 1). In addition, prior studies in our lab have established that basal levels of HSP70 protein abundance were not significantly altered by SO. Therefore, SO studies were not replicated (23).

Lung Isolation

Following exsanguinations, each lung was removed and gently perfused with fixative (Tissue-Tek OCT Compound, Electron Microscopy Sciences, Hatfield, PA). Individual lobes were separated from each other and some were flash frozen in liquid nitrogen. 5μm sections were prepared, adhered to glass slides and stored at - 80°C until analysis. The remaining lobes were removed en bloc, gently perfused with 0.9% saline, homogenized and protein was extracted.

Whole Lung Protein Extract

Homogenization for protein was conducted as previously described (38). The final protein extract was filtered through an Amicon Ultra-4 50K Centrifugal Filter Device (Merck Millipore, Billerica, MA) to maximize recovery. Protein concentration for each sample was determined using the Microplate BCA Protein Assay Kit (Thermo Scientific, Rockford, IL).

Immunohistochemistry and Quantification of HSP70 and MPO Abundance in Lung Parenchyma

Lung sections were thawed and incubated with blocking buffer (Starting Block, Thermo Fisher Scientific Inc., Rockford, IL) and then fixed in 10% buffered formalin. HSP70 abundance was determined using a 1:100 dilution of a goat polyclonal (SC 1060, Santa Cruz Biotechnology, Inc., Dallas, TX). Myeloperoxidase (MPO) abundance was assessed using a 1:100 dilution of a rabbit polyclonal antibody to MPO (SC 33596, Santa Cruz Biotechnology, Inc., Dallas, TX). The secondary antibody was a 1:800 dilution of a donkey anti-goat coupled to Alexa Fluor 555 (Invitrogen/Life Technologies, Grand Island, NY) and Alexa Fluor 555 goat anti-rabbit (Invitrogen/Life Technologies, Grand Island, NY). Sections were incubated with 4',6-diamidino-2-phenylindole (DAPI) to allow visualization of cell nuclei (Molecular Probes, Eugene, OR). Similar incubation and staining were performed on samples of human malignant lung tissue (tissue samples were provided by the Cooperative Human Tissue Network, Department of Pathology and Lab Medicine at the University of Pennsylvania and approved for research purposes by Penn IRB and the National Cancer Institute, National Institutes of Health) that provided positive and negative controls for the HSP70 antibody (39, 40). Fluorescent mounting medium from KPL (Gaithersburg, MD) was added prior to microscopic examination. Fluorescence was quantified using the iVision for Macintosh Scientific Image Processing program, (iVision 4.0.14, Biovision Technologies, Chester Springs, PA). The total number of nucleated cells positive for HSP70 and the number of DAPI-positive cells per high-powered field were counted. The mean fluorescence intensity of MPO per cell was calculated. Cell counts on ten randomly-chosen high-powered fields per lung lobe section per rat were assessed, counted and averaged.

Determination of MIP-2 and CINC-1 Protein Activity

Abundance of MIP-2 and CINC-1 protein in whole lung homogenate was measured by Enzyme-Linked Immunosorbent Assays (Rat GRO–β/MIP–2, Antigenix America, Huntington Station, NY, and Rat CXCL1/CINC-1, R&D Systems, Minneapolis, MN). The inter-assay coefficient of variation was 10 %.

Lung Histology and Morphology

Lung sections were stained with hematoxylin and eosin (H&E) and evaluated by a veterinary pathologist blinded to procedure and intervention. Evidence of minimal, mild, moderate or marked neutrophil score (neutrophil count of 0-15, 15-25, 25-50, >50 respectively), and normal or abnormal changes consistent with ARDS were assessed using the following criteria: location of lesion, septal thickening, amount of interstitial proteinacious material (fibrin/edema), alveolar collapse (or areas containing alveolar histiocytes, eosinophils and mast cells), hyaline membrane and presence of lymphocytes. In addition, the percentage of inflamed areas, calculated by the criteria listed above, per lobe was quantified using a computer algorithm (Aperio Image Scope program, v11.0.2.725 for PC, Pathology Core Laboratory, Children's Hospital of Philadelphia Research Institute, Philadelphia, PA).

Statistical Analysis

Our primary outcome variables were indices of lung injury – histology score, MPO (and, by extension, neutrophil) abundance and chemokine expression. Previous studies focusing on the same variables have required the study of three animals per time point (all four papers on AdHSP). Therefore, as requested by our IACUC, we used this same approach to limit the number of animals required for this study. We made provisions to investigate additional animals should there be a suspicion of beta error. The significance of differences in protein abundance in lung homogenate as a function of time and intervention was determined using two-tailed ANOVA with a Bonferroni correction. For survival studies Kaplan Meier and Cox proportional hazard regression analyses were performed. Significance was set at $p < 0.05$. A general linear model, allowing for the inclusion of data from all time points, was used for the statistical analysis assuming equal variance in order to further maximize statistical power.

Results

Intra-tracheal administration of TAT-HSP70 increased HSP70 protein abundance in the lungs following CLP

We show stable bacterial protein expression of recombinant TAT-HSP70 used in our experiments (Fig. 1A). Positive and negative controls for HSP70 antibody are shown in Figs. 1C and E, and Figs. B and D, respectively. We first determined the effect of TAT-HSP70 administration on HSP70 abundance in the lungs. There was no statistically significant difference in the abundance of HSP70 in untreated (T0) controls (Fig. 1E) or in animals studied at either 24 (Fig. 1F) or 48 h (Fig. 1H) following CLP (Fig. 1). In contrast, treatment with TAT-HSP70 significantly increased HSP70 abundance at 24 (Fig. 1G) and 48 h (Fig. 1I) after CLP relative to both T0 and to abundance in CLP animals treated with PBS (Fig. 1J).

Intra-tracheal administration of TAT-HSP70 increased HSP70 protein abundance in abnormal and normal lung sections following CLP

Lung damage in ARDS is heterogenous and falls on spectrum of severity from un-altered to severely abnormal. The pathologic changes include septal thickening, accumulation of interstitial proteinacious material (fibrin/edema), alveolar collapse, presence of hyaline membrane and enhanced abundance of lymphocytes and neutrophils.

To determine if TAT-HSP70 preferentially affected normal or abnormal lung regions, we examined the effects of CLP and treatment on HSP70 abundance in random sections of whole lung lobes. TAT-HSP70 increased HSP70 abundance in both normal and abnormal lung regions at both 24 and 48 h after CLP. The increases in HSP70 abundance as a function of time from intervention or histologic abnormality did not differ significantly from each other (data not shown).

Intra-tracheal administration of TAT-HSP70 attenuated histologic findings of lung injury following CLP

Prior work has shown that augmenting HSP70 abundance ameliorated histologic evidence of lung injury following CLP (24). To determine if this was also the case using the TAT delivery system, we examined representative lung lobe sections. When compared to samples from T0 rats (Fig. 2A), lung histology and architecture became progressively more abnormal in CLP rats treated with PBS (Figs. 2B and 2D). In contrast, at both 24 and 48 h following CLP, lung injury was minimal in rats treated with TAT-HSP70 (Figs. 2C and E). Thus, treatment with TATHSP70 limited CLP-induced lung injury.

Intra-tracheal administration of TAT-HSP70 decreased MPO abundance at 48 hours following CLP

Previous studies have shown that increasing HSP70 abundance following CLP limited neutrophil infiltration into lung tissue. To determine whether improved lung histology was associated with decreased neutrophil influx, we examined lung MPO levels using immunohistochemistry. Treatment with PBS did not significantly alter CLP-induced MPO abundance at 24 h (Figs. 3B1 and 3B2). When compared to PBS treatment, administration of TAT-HSP70 did not significantly alter MPO abundance 24 h after CLP (Figs. 3C1 and 3C2). However, relative to treatment with PBS (Figs. 3D1 and 3D2), TAT-HSP70 administration significantly reduced MPO abundance 48 h after CLP (Figs. 3E1, 3E2 and 3F).

TAT-HSP70 administration decreased whole lung protein abundance of MIP-2 and CINC-1 at 24 hours following CLP

Sepsis-induced increases in pulmonary neutrophil infiltration are mediated, in part, by chemokines, most notably MIP-2 and CINC-1. To determine the effects of TAT-HSP70 on MIP-2 and CINC-1 protein abundance, we analyzed levels in homogenized lung tissue. MIP-2 and CINC-1 protein abundance were significantly increased at 24 h following CLP in PBS-treated rats (Figs. 4 and 5). Treatment with TAT-HSP70, however, significantly reduced CLP-induced increases in MIP-2 and CINC-1 levels at 24 h following CLP. Changes in pulmonary levels of CINC-1 and MIP-2 were not sustained at 48 hours.

TAT-HSP70 administration increased survival at 48 hours following CLP

To determine if TAT-HSP70 had an effect on survival, we analyzed mortality at the designated 24 and 48 h time points (Fig. 6). There was a 65% survival rate in rats subjected to CLP and treated with PBS at 48 h. In contrast, 86% of the septic rats that received TAT-HSP70 survived to 48 h (p = 0.09). Thus, treatment with TAT-HSP70 resulted in a trend for the CLPTAT-HSP70 treated rats to survive at 48 h.

Discussion

The data presented here demonstrate that use of the TAT peptide is an effective way to increase the abundance of HSP70 in the lungs of rats subjected to CLP. This increase in HSP70 was associated with reduced histologic lung injury, decreased neutrophil infiltration and an early reduction in MIP-2 and CINC-1 expression. While the study was not powered to examine mortality, we also observed a trend towards improved survival at 48 h.

Previous studies have shown that enhancing HSP70 abundance in rats with ARDS secondary to CLP improved a number of parameters (24, 26-28). However, these studies introduced HSP70 using an adenoviral vector. This approach relies upon use of an infective agent and requires that the mechanisms mediating endogenous gene expression remain intact. Therefore, we sought an alternative approach. The TAT protein has been used to increase protein abundance in a number of settings, including this same model of ARDS, and thus seems a logical choice. Our data do indeed indicate this method can be used successfully. We also were able to demonstrate that, TAT-mediated transduction protein resulted in uniform distribution of HSP70 throughout the lung, a finding we have not previously demonstrated.

Neutrophils are believed to play an important role in the development of the lung injury that characterizes ARDS and, indeed neutrophil abundance in the lung increases following CLP (35, 36, 41). In rats, neutrophil accumulation is primarily mediated by the chemotactic proteins, CINC-1 and MIP-2, which performs a function similar to that of IL-8 in humans. CINC-1 and MIP-2 levels increased in response to CLP, peaking at 24 h and then decreasing. Administration of TAT-HSP70 significantly reduced pulmonary levels of both CINC-1 and MIP-2 at 24 h. The increase was not sustained to 48 hours, a finding consistent with a decrease in neutrophil infiltration, as demonstrated by a decrease in MPO.

The mechanisms by which TAT and its cargo protein enter cells remain unknown. Studies to date are inconclusive but suggest intracellular localization through macropinocytosis, clathrin-mediated endocytosis or the formation of lipid rafts through caveolae processes (33, 34). Specific characteristics of the TAT protein that are favorable to cargo peptide or protein transduction include TAT's highly cationic, arginine and lysine-rich structure facilitating transduction through the hydrophobic lipid bilayer and negatively charged cell membrane.

Our previous work has suggested several mechanisms by which intracellular HSP70 protein abundance might reduce indirect lung injury (24, 26-28). These include limiting NF-κB activation, preservation of pulmonary epithelial alveolar Type I cells, attenuated proliferation of Type II cells and impairment of apoptotic cellular pathways. Given the

similarities between the changes reported here and those observed in studies where HSP70 was delivered using an adenoviral vector, it is logical that the same mechanisms are operant.

Our study has significant limitations that have important ramifications. We used a single dose of TAT-HSP70 and administered it at the time of CLP. Clearly this cannot be done in clinical practice. Additional experiments to establish the therapeutic window for TAT-HSP70 are clearly warranted. Further, we selected a dose of 100μg based on pilot studies. Generation of a dose – response curve would be an important future project. Conversely, we used a single dose. TAT-HSP70 could be given several times to an individual patient. We examined the effects of our outcomes at two pre-determined time-points. The study was not appropriately powered to examine outcome and a survival study would be important. Finally, recent studies have questioned the validity and generalizability of findings from CLP studies in mice to the human syndrome. Indeed, a litany of factors must be considered prior to extrapolating animal data to clinical human syndromes (42). None-the-less, the use of low tidal-volume ventilation is the only treatment to decrease mortality and hospital length of stay in human ARDS (20, 43-45). Therefore, exploration of a potentially viable approach, such as the use of TAT-HSP70, must be considered.

In conclusion, we have demonstrated that increasing HSP70 using the TAT-protein system is a viable delivery mechanism with which to approach treatment of CLP-induced ARDS in rats. Future studies will seek to optimize the use of TAT-HSP70 as a treatment for lung injury secondary to sepsis.

Acknowledgments

References

1. Angus DC, van der Poll T. Severe sepsis and septic shock. N Engl J Med. 2013; 369(9):840–851. [PubMed: 23984731]

2. Hoyert DL, Xu JQ. Deaths: Preliminary data for 2011. National vital statistics reports. NCHS Data Brief. 2012; 61(6)

3. Vincent JL, Sakr Y, Sprung CL, Ranieri VM, Reinhart K, Gerlach H, et al. Sepsis in European intensive care units: results of the SOAP study. Crit Care Med. 2006; 34(2):344–353. [PubMed: 16424713]

4. Gaieski DF, Edwards JM, Kallan MJ, Carr BG. Benchmarking the incidence and mortality of severe sepsis in the United States. Crit Care Med. 2013; 41(5):1167–1174. [PubMed: 23442987]

5. Griffiths RD, Hall JB. Intensive care unit-acquired weakness. Crit Care Med. 2010; 38(3):779–787. [PubMed: 20048676]

6. Iwashyna TJ, Ely EW, Smith DM, Langa KM. Long-term cognitive impairment and functional disability among survivors of severe sepsis. JAMA. 2010; 304(16):1787–1794. [PubMed: 20978258]

7. Yende S, Angus DC. Long-term outcomes from sepsis. Curr Infect Dis Rep. 2007; 9(5):382–386. [PubMed: 17880848]

8. Iwashyna TJ, Cooke CR, Wunsch H, Kahn JM. Population burden of long-term survivorship after severe sepsis in older Americans. J Am Geriatr Soc. 2012; 60(6):1070–1077. [PubMed: 22642542]

9. Angus DC, Linde-Zwirble WT, Lidicker J, Clermont G, Carcillo J, Pinsky MR. Epidemiology of severe sepsis in the United States: analysis of incidence, outcome, and associated costs of care. Crit Care Med. 2001; 29(7):1303–1310. [PubMed: 11445675]

10. Deutschman CS, Tracey KJ. Sepsis: current dogma and new perspectives. Immunity. 2014; 40(4): 463–475. [PubMed: 24745331]

11. Hotchkiss RS, Monneret G, Payen D. Sepsis-induced immunosuppression: from cellular dysfunctions to immunotherapy. Nat Rev Immunol. 2013; 13(12):862–874. [PubMed: 24232462]

12. Lagu T, Rothberg MB, Shieh MS, Pekow PS, Steingrub JS, Lindenauer PK. Hospitalizations, costs, and outcomes of severe sepsis in the United States 2003 to 2007. Crit Care Med. 2012; 40(3):754–761. [PubMed: 21963582]

13. Force ADT, Ranieri VM, Rubenfeld GD, Thompson BT, Ferguson ND, Caldwell E, et al. Acute respiratory distress syndrome: the Berlin Definition. JAMA. 2012; 307(23):2526–2533. [PubMed: 22797452]

14. Perl M, Lomas-Neira J, Venet F, Chung CS, Ayala A. Pathogenesis of indirect (secondary) acute lung injury. Expert Rev Respir Med. 2011; 5(1):115–126. [PubMed: 21348592]

15. Baumann H, Gauldie J. The acute phase response. Immunol Today. 1994; 15(2):74–80. [PubMed: 7512342]

16. Grommes J, Soehnlein O. Contribution of neutrophils to acute lung injury. Mol Med. 2011; 17(3-4):293–307. [PubMed: 21046059]

17. Kellum JA, Kong L, Fink MP, Weissfeld LA, Yealy DM, Pinsky MR, et al. Understanding the inflammatory cytokine response in pneumonia and sepsis: results of the Genetic and Inflammatory Markers of Sepsis (GenIMS) Study. Arch Intern Med. 2007; 167(15):1655–1663. [PubMed: 17698689]

18. Matthay MA, Ware LB, Zimmerman GA. The acute respiratory distress syndrome. J Clin Invest. 2012; 122(8):2731–2740. [PubMed: 22850883]

19. Thille AW, Esteban A, Fernandez-Segoviano P, Rodriguez JM, Aramburu JA, Penuelas O, et al. Comparison of the Berlin definition for acute respiratory distress syndrome with autopsy. Am J Respir Crit Care Med. 2013; 187(7):761–767. [PubMed: 23370917]

20. (ARDSNET). ARDSN: Ventilation with lower tidal volumes as compared with traditional tidal volumes for acute lung injury and the acute respiratory distress syndrome. The Acute Respiratory Distress Syndrome Network. N Engl J Med. 2000; 342(18):1301–1308. [PubMed: 10793162]

21. Herridge MS, Tansey CM, Matte A, Tomlinson G, Diaz-Granados N, Cooper A, et al. Functional disability 5 years after acute respiratory distress syndrome. N Engl J Med. 2011; 364(14):1293–1304. [PubMed: 21470008]

22. Lindquist S, Craig EA. The heat-shock proteins. Annu Rev Genet. 1988; 22:631–677. [PubMed: 2853609]

23. Weiss YG, Bouwman A, Gehan B, Schears G, Raj N, Deutschman CS. Cecal ligation and double puncture impairs heat shock protein 70 (HSP-70) expression in the lungs of rats. Shock. 2000; 13(1):19–23. [PubMed: 10638664]

24. Weiss YG, Maloyan A, Tazelaar J, Raj N, Deutschman CS. Adenoviral transfer of HSP-70 into pulmonary epithelium ameliorates experimental acute respiratory distress syndrome. J Clin Invest. 2002; 110(6):801–806. [PubMed: 12235111]

25. Weiss YG, Tazelaar J, Gehan BA, Bouwman A, Christofidou-Solomidou M, Yu QC, et al. Adenoviral vector transfection into the pulmonary epithelium after cecal ligation and puncture in rats. Anesthesiology. 2001; 95(4):974–982. [PubMed: 11605941]

26. Aschkenasy G, Bromberg Z, Raj N, Deutschman CS, Weiss YG. Enhanced Hsp70 expression protects against acute lung injury by modulating apoptotic pathways. PLoS One. 2011; 6(11):e26956. [PubMed: 22132083]

27. Bromberg Z, Raj N, Goloubinoff P, Deutschman CS, Weiss YG. Enhanced expression of 70-kilodalton heat shock protein limits cell division in a sepsis-induced model of acute respiratory distress syndrome. Crit Care Med. 2008; 36(1):246–255. [PubMed: 17989570]

28. Weiss YG, Bromberg Z, Raj N, Raphael J, Goloubinoff P, Ben-Neriah Y, et al. Enhanced heat shock protein 70 expression alters proteasomal degradation of IkappaB kinase in experimental acute respiratory distress syndrome. Crit Care Med. 2007; 35(9):2128–2138. [PubMed: 17855826]

29. Sheridan C. Gene therapy finds its niche. Nat Biotechnol. 2011; 29(2):121–128. [PubMed: 21301435]

30. Frankel AD, Pabo CO. Cellular uptake of the tat protein from human immunodeficiency virus. Cell. 1988; 55(6):1189–1193. [PubMed: 2849510]

31. Green M, Loewenstein PM. Autonomous functional domains of chemically synthesized human immunodeficiency virus tat trans-activator protein. Cell. 1988; 55(6):1179–1188. [PubMed: 2849509]

32. Doeppner TR, Kaltwasser B, Fengyan J, Hermann DM, Bahr M. TAT-Hsp70 induces neuroprotection against stroke via anti-inflammatory actions providing appropriate cellular microenvironment for transplantation of neural precursor cells. J Cereb Blood Flow Metab. 2013; 33(11):1778–1788. [PubMed: 23881248]

33. Gump JM, Dowdy SF. TAT transduction: the molecular mechanism and therapeutic prospects. Trends Mol Med. 2007; 13(10):443–448. [PubMed: 17913584]

34. Heitz F, Morris MC, Divita G. Twenty years of cell-penetrating peptides: from molecular mechanisms to therapeutics. Br J Pharmacol. 2009; 157(2):195–206. [PubMed: 19309362]

35. Kilpatrick LE, Standage SW, Li H, Raj NR, Korchak HM, Wolfson MR, et al. Protection against sepsis-induced lung injury by selective inhibition of protein kinase C-delta (delta-PKC). J Leukoc Biol. 2011; 89(1):3–10. [PubMed: 20724665]

36. Mondrinos MJ, Zhang T, Sun S, Kennedy PA, King DJ, Wolfson MR, et al. Pulmonary endothelial protein kinase C-delta (PKCdelta) regulates neutrophil migration in acute lung inflammation. Am J Pathol. 2014; 184(1):200–213. [PubMed: 24211111]

37. Wheeler DS, Dunsmore KE, Wong HR. Intracellular delivery of HSP70 using HIV-1 Tat protein transduction domain. Biochem Biophys Res Commun. 2003; 301(1):54–59. [PubMed: 12535640]

38. Abcejo AS, Andrejko KM, Raj NR, Deutschman CS. Failed interleukin-6 signal transduction in murine sepsis: attenuation of hepatic glycoprotein 130 phosphorylation. Crit Care Med. 2009; 37(5):1729–1734. [PubMed: 19325483]

39. Asea A, Kraeft SK, Kurt-Jones EA, Stevenson MA, Chen LB, Finberg RW, et al. HSP70 stimulates cytokine production through a CD14-dependant pathway, demonstrating its dual role as a chaperone and cytokine. Nat Med. 2000; 6(4):435–442. [PubMed: 10742151]

40. Daugaard M, Rohde M, Jaattela M. The heat shock protein 70 family: Highly homologous proteins with overlapping and distinct functions. FEBS Lett. 2007; 581(19):3702–3710. [PubMed: 17544402]

41. Guo RF, Riedemann NC, Sun L, Gao H, Shi KX, Reuben JS, et al. Divergent signaling pathways in phagocytic cells during sepsis. J Immunol. 2006; 177(2):1306–1313. [PubMed: 16818791]

42. Seok J, Warren HS, Cuenca AG, Mindrinos MN, Baker HV, Xu W, et al. Genomic responses in mouse models poorly mimic human inflammatory diseases. Proc Natl Acad Sci U S A. 2013; 110(9):3507–3512. [PubMed: 23401516]

43. Thompson BT, Bernard GR. ARDS Network (NHLBI) studies: successes and challenges in ARDS clinical research. Crit Care Clin. 2011; 27(3):459–468. [PubMed: 21742211]

44. Opal SM, Laterre PF, Francois B, LaRosa SP, Angus DC, Mira JP, et al. Effect of eritoran, an antagonist of MD2-TLR4, on mortality in patients with severe sepsis: the ACCESS randomized trial. JAMA. 2013; 309(11):1154–1162. [PubMed: 23512062]

45. Ranieri VM, Thompson BT, Barie PS, Dhainaut JF, Douglas IS, Finfer S, et al. Drotrecogin alfa (activated) in adults with septic shock. N Engl J Med. 2012; 366(22):2055–2064. [PubMed: 22616830]
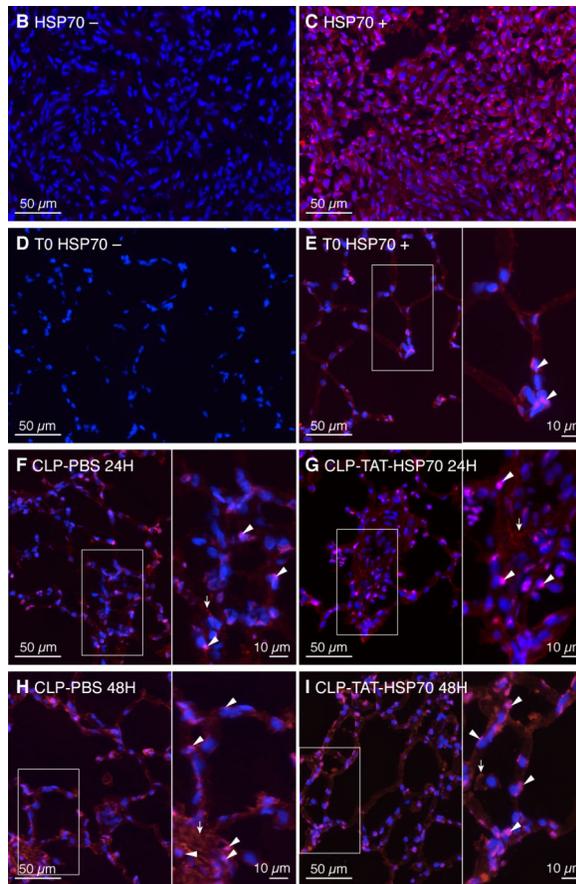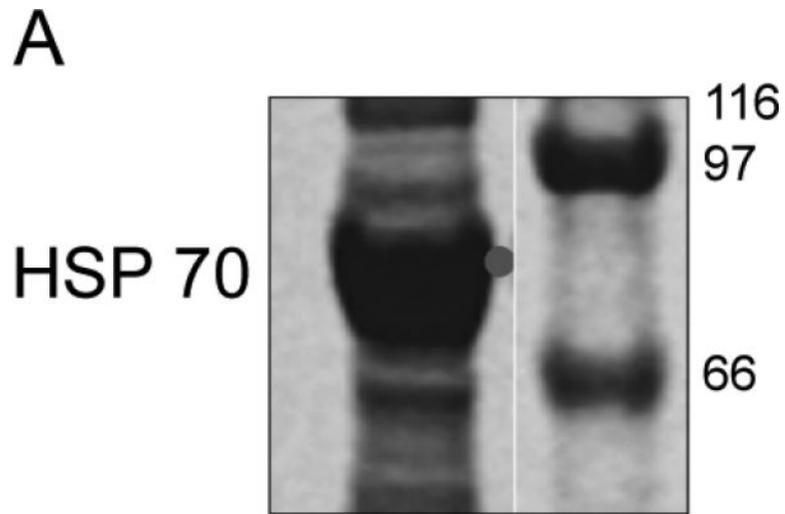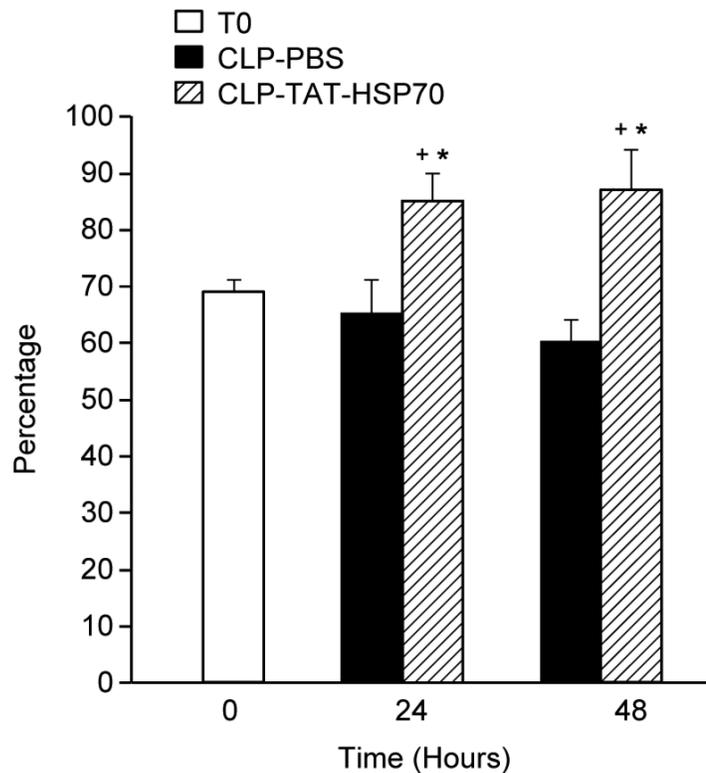
Figure 1. Immunohistochemistry analysis of HSP70 protein within the cytoplasm of lung alveolar sections

Top (A): Coomassie - stained protein gel showing stable bacterial protein expression of TAT-HSP70. Middle (B-C): Representative sections from control human lung tissue. HSP70 staining appears magenta. Nuclei stained with DAPI appear blue. (B) Negative Control - section of human lung tissue containing malignancy stained w/o anti-HSP70, (C) Positive Control - section of human lung tissue containing malignancy expressing abundance of HSP70 stained with anti- HSP70. Middle (D-I): Representative sections from rat lung tissue, T0, CLP-PBS treated and CLP-TAT-HSP70 treated animals at 24 and 48 h. (D) Antibody Control – sections from T0 rat not treated with anti-HSP70 and (E) treated with HSP70 antibody, (F) Sections from CLP-PBS rats at 24 h and comparison, (G) section from CLP-TAT-HSP70 treated rats at 24 h, (H) sections from CLP-PBS rats at 48 h and comparison, (I) section from CLP-TAT-HSP70 treated rats at 48 h. Magnifications at 20X. Scale bars – 50 μm in B-I; additionally, scale bars of image inserts – 10 μm to the right of select images as illustrated. Arrow = HSP70 staining appears magenta around nuclei. Arrowhead = not HSP70. Bottom (J): Graphic comparison (mean ± Standard Error (SE)) of HSP70 absorbance ratios in lung sections. y-axis: fraction of HSP70 abundance in the cytoplasm per nuclei/high-powered field. x-axis: time (hours). Counts from 10 high-powered fields /slide, one slide/animal. $*$ = P<0.05 compared to T0, $+$ = P<0.05 compared to CLP-PBS at the same time point. n = three surviving rats/interventional group.
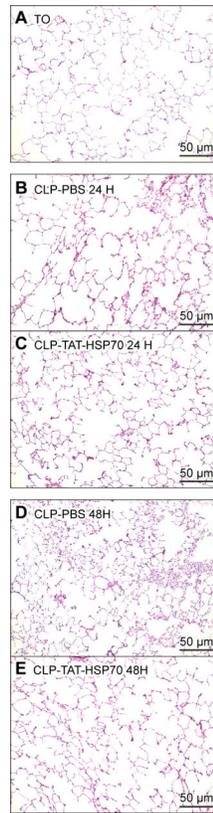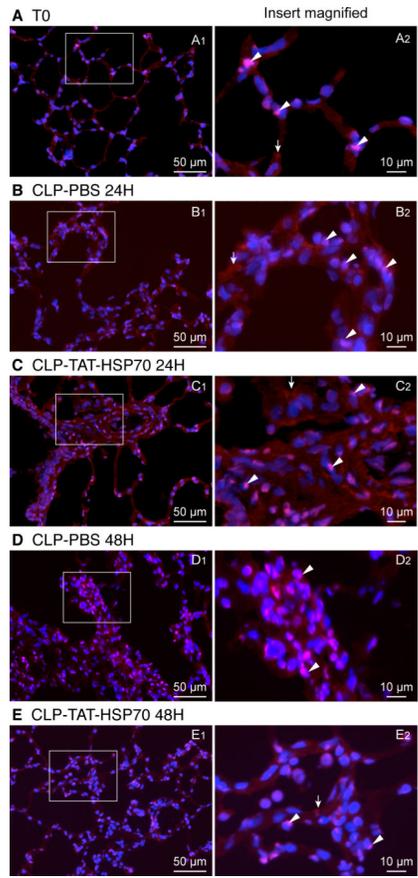
Figure 2. Histologic lung injury following CLP

H&E staining of lung sections obtained from rats at T0 (A), CLP-PBS treated animals at 24 (B) and 48 h (D), and CLP-TAT-HSP70 treated animals at 24 (C) and 48 h (E). 20X magnification. Scale bars – 50 μm.
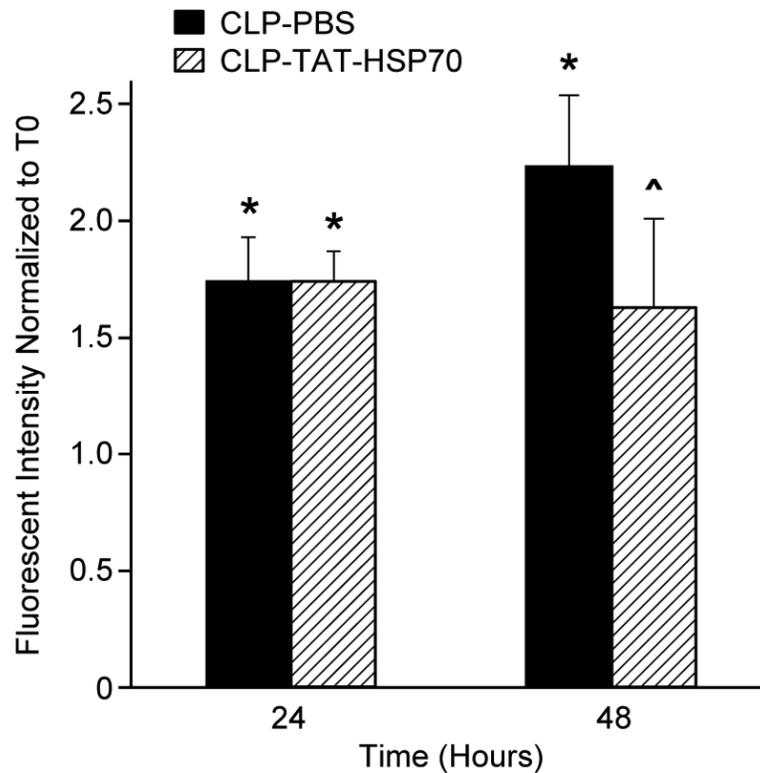
Figure 3. Immunohistochemistry analysis of MPO protein within the cytoplasm of lung alveolar sections

Top (A-E): Representative sections from control (T0), CLP-PBS treated and CLP-TAT-HSP70 treated animals at 24 and 48 h. Blue staining – DAPI in nuclei. Magenta staining – nuclei double labeled with both MPO and DAPI. 20X magnification. Scale bars – 50 μm on the left (A1-E1); magnification of image inserts – 10 μm on the right (A2-E2). Arrow = HSP70 staining appears magenta around nuclei. Arrowhead = not HSP70. Bottom (F): Graphic comparison (mean ± SE) of MPO fluorescence intensity ratios in lung sections. y-axis - MPO fluorescence intensity normalized to T0 (1). x-axis - time (hours). Counts performed on 10 randomly selected lung sections/high-power field, one slide/animal. * = P<0.05 compared to T0, ^ = P<0.05 compared to CLP-PBS at the same time point. n = 3 surviving rats/intervention group..
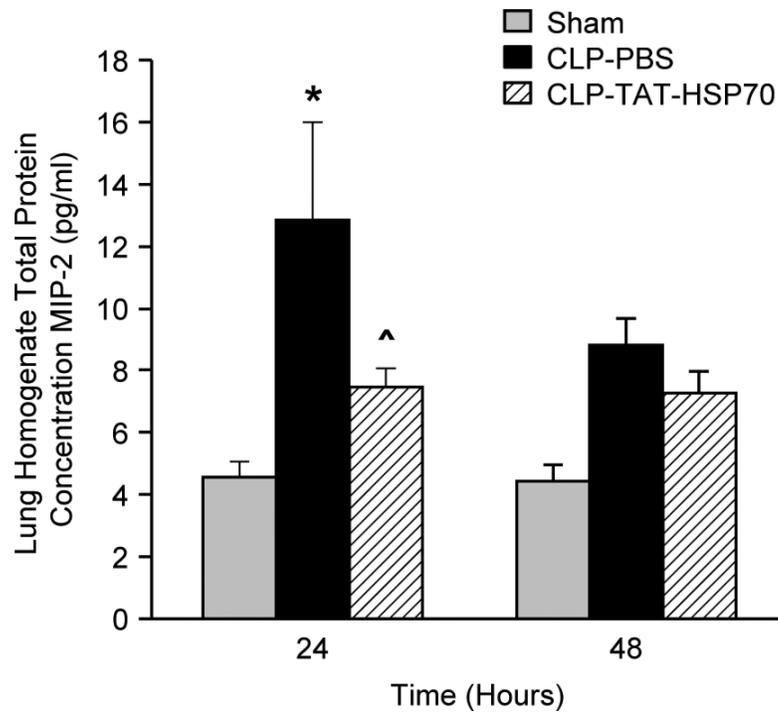
Figure 4. Whole lung protein levels of MIP-2 following CLP at 24 and 48 h
Graphic comparison (mean ± SE) of MIP-2 abundance in lung regions. The y axis shows MIP-2 abundance in lung homogenate. The x axis shows time in hours. Graph reflects, SO 24 (n=6), CLP-PBS 24 (n=8), CLP-TAT-HSP70 24 (n=9), SO 48 (n=4), CLP-PBS 48 (n=8), CLP-TAT HSP70 48 (n=8). * = P<0.05 compared to SO at the same time point, ^ = P<0.05 compared to CLP-PBS at the same time point.
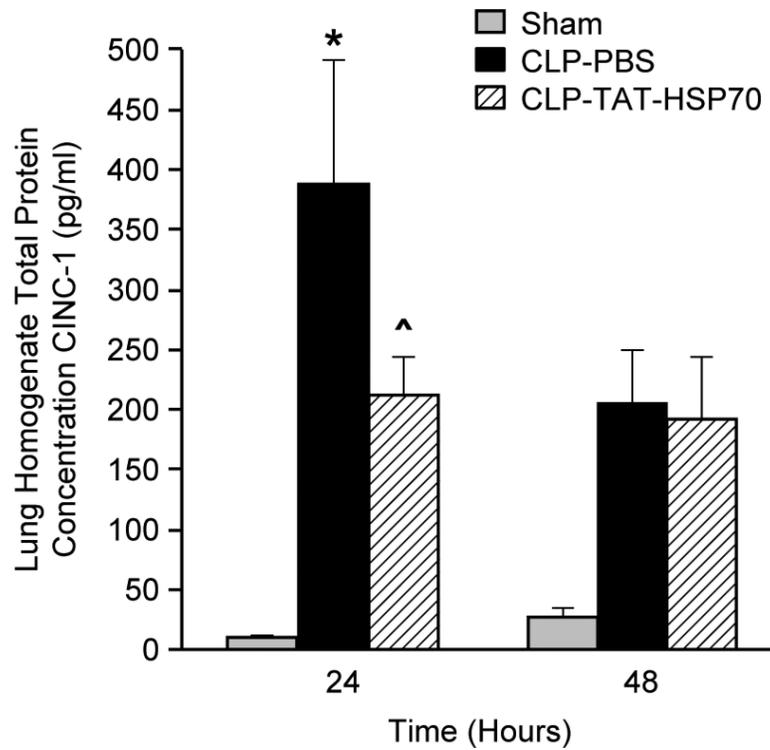
Figure 5. Whole lung protein levels of CINC-1 following CLP at 24 and 48 h

Graphic comparison (mean ± SE) of CINC-1 abundance in lung regions. Graph reflects, SO 24 (n=6), CLP-PBS 24 (n=6), CLP-TAT-HSP70 24 (n=9), SO 48 (n=4), CLP-PBS 48 (n=7), CLP-TAT-HSP70 48 (n=7). * = P<0.05 compared to SO at same time point, ^ = P<0.05 compared to CLP-PBS at the same time point.
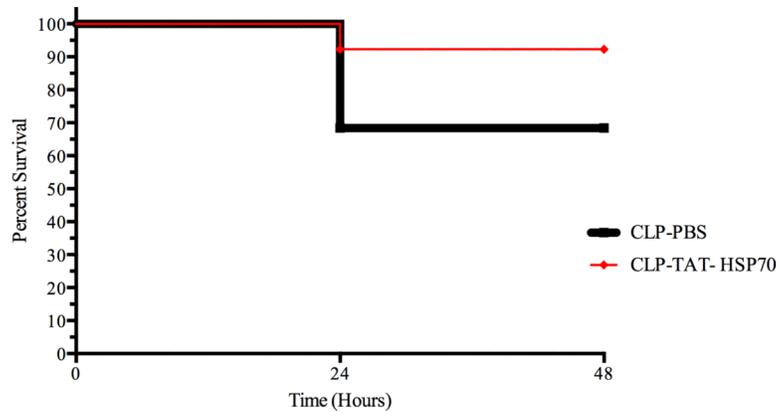
Figure 6.
Kaplan Meier survival analysis of T0, CLP-PBS and CLP-TAT-HSP70 rats at 24 and 48 h.
We observed mortality of 10% in both CLP-PBS and CLP-TAT-HSP70 rat groups at 24 h,
mortality of 35% in the CLP-PBS rats at 48 h and mortality of 14% in the CLP-TAT-HSP70
rats at the similar time point (p=0.09), indicating a trend toward survival in the CLP-TAT-
HSP70 48 h group. Number of rats per group, T0 (n=3), CLP-PBS 24 (n=11), CLP-TAT-
HSP70 24 (n=12), CLP-PBS 48 (n= 20), CLP-TAT-HSP70 48 (n= 14).

Table 1

Numbers of Sprague Dawley Rats[*]

Group	Description	# Animals
T0	Unoperated Controls	3
SO	Subjected to Sham Operation	13
CLP-TAT-HSP70	CLP with two 18-g punctures + TAT-HSP70	26
CLP-PBS	CLP with two 18-g punctures + PBS only	31

* Survival was not the same in each group of animals. Therefore, different numbers of animals were required to obtain three survivors.